minerals

MDPI

Article

Immobilisation of Platinum by *Cupriavidus metallidurans*

Gordon Campbell [1], Lachlan MacLean [2], Frank Reith [3,4], Dale Brewe [5], Robert A. Gordon [5] and Gordon Southam [6,*]

1 Department of Earth Sciences, The University of Western Ontario, London, ON N6A 5B7, Canada; s.gordon.campbell@ualberta.ca
2 Canadian Light Source, Saskatoon, SK S7N 2V3, Canada; lcwmaclean@gmail.com
3 School of Biological Sciences, The Sprigg Geobiology Centre, The University of Adelaide, School of Biological Sciences, Adelaide, SA 5005, Australia; frank.reith@adelaide.edu.au
4 CSIRO Land and Water, Environmental Contaminant Mitigation and Technologies, PMB2, Glen Osmond, SA 5064, Australia
5 Pacific Northwest Consortium Synchrotron Radiation Facility, Advanced Photon Source, Argonne, IL 60439, USA; brewe@aps.anl.gov (D.B.); ragordon@alumni.sfu.ca (R.A.G.)
6 School of Earth and Environmental Sciences, The University of Queensland, St. Lucia, QLD 4072, Australia
* Correspondence: g.southam@uq.edu.au; Tel.: +61-7-3365-8505

Received: 1 December 2017; Accepted: 26 December 2017; Published: 5 January 2018

Abstract: The metal resistant bacterium *Cupriavidus metallidurans* CH34, challenged with aqueous platinous and platinic chloride, rapidly immobilized platinum. XANES/EXAFS analysis of these reaction systems demonstrated that platinum binding shifted from chloride to carboxyl functional groups within the bacteria. Pt(IV) was more toxic than Pt(II), presumably due to the oxidative stress imparted by the platinic form. Platinum immobilisation increased with time and with increasing concentrations of platinum. From a bacterial perspective, intracellular platinum concentrations were two to three orders of magnitude greater than the fluid phase, and became saturated at almost molar concentrations in both reaction systems. TEM revealed that *C. metallidurans* was also able to precipitate nm-scale colloidal platinum, primarily along the cell envelope where energy generation/electron transport occurs. Cells enriched in platinum shed outer membrane vesicles that were enriched in metallic, colloidal platinum, likely representing an important detoxification strategy. The formation of organo-platinum compounds and membrane encapsulated nanophase platinum, supports a role for bacteria in the formation and transport of platinum in natural systems, forming dispersion halos important to metal exploration.

Keywords: geomicrobiology; platinum; *Cupriavidus metallidurans*; biomineralisation; synchrotron

1. Introduction

Microorganisms are able to thrive under a variety of extreme conditions including strongly acidified soils and metal-rich mineralized zones [1–3]. Some metal-tolerant bacteria in these environments are able to carve out niche existences by using the available metal and metal-containing compounds as sources of nutrition and energy [4]. Alternatively, some bacteria may invoke genetically encoded detoxification mechanisms to mitigate the effects of high metal concentrations [5]. These steps can involve metal reduction, complexation, precipitation, efflux or a combination thereof [6,7].

The biogeochemical cycling of precious metals and the formation of certain geologic deposits can be attributed to microbial activity [8–12]. In vitro studies have shown that bacteria are able to immobilize and/or precipitate gold from gold-rich solutions [13–16]. Kenney et al. [17] noted that non-metabolizing bacteria were also able to remove gold from aqueous gold solutions.

The morphologies of bio-precipitated gold so closely resemble the gold found in contemporary (Australia) and paleoplacers, e.g., South Africa's Witwatersrand basin, that a biogenic origin for these auriferous deposits [8,9,18,19] is now accepted.

The chemical properties that give gold the ability be part of a biogeochemical pathway are not necessarily unique to that element. In fact, gold shares similar properties to platinum. Like gold, platinum is a chalcophile element, as it preferentially forms covalent bonds with sulphur [20]. As such, platinum and gold share similar transport mechanisms in the crust and can be deposited in both magmatic and hydrothermal systems. In some polymetallic deposits, gold and platinum are alloyed to one another [21,22]. The question remains: does this similar geochemical behaviour extend to low temperature, i.e., Earth surface weathering conditions? Recent work on placer platinum grains indicates that weathering, including the biogeochemical cycling of platinum does occur, albeit to a much lesser extent than gold [23–25].

Platinum, one of the six platinum group elements, is a highly valued metal [26,27]. Its concentration in the lithosphere is scarce, but it can reach economic concentrations in primary and secondary ore deposits [22,28]. Under surficial weathering conditions, the predicted oxidation state of platinum in aqueous solutions is Pt(II) or Pt(IV) [29]. Based on thermodynamic calculations, platinum is likely to occur as free aqueous ions only in oxidising and acidic environments, therefore, under most surficial conditions, platinum occurs as stable colloids/nanoparticles or is bound by coordination complexes to organic and inorganic ligands [29–32].

Platinum commonly forms complexes with chlorides, hydroxides and thiosulphates, but amorphous organo-platinum and platinum-hydroxide colloids also occur [29,30,32–36]. Aqueous platinum is transported in the surficial environment until conditions favour its (biogeo)chemical transformation and/or chemical precipitation. Subsequent migration and deposition of platiniferous material may occur [32,37]. While these processes were assumed to be primarily abiotic, recent research has shown that bacteria-mediated platinum immobilisation may also contribute to the formation of platinum placer grains [15,25].

Lengke et al. [38] demonstrated that cyanobacteria are able to reduce aqueous Pt(IV) species in a stepwise reaction that first produces intracellular and extracellular spherical platinum (II) organic nano-condensates. The amorphous platinum (II) colloids then experienced further diagenesis to produce crystalline, elemental platinum. Platinum can also be reduced by the metal reducing bacterium *Shewanella algae* [39]. These experimental findings are supported by the recent discovery and characterisation of small alluvial platinum grains with morphologies characteristic of platinum-encrusted bacteria [40]. Microbes attached to an organic substrate, i.e., a decaying plant root, precipitated platinum from solution onto their surface. In this system, it is thought that continued bioreduction and subsequent electrochemical accretion of platiniferous nanoparticles likely contributed to the formation of the biogenic alluvial grains [40].

Further investigation is still needed to understand the specific role(s) that microbes play in platinum biomineralisation [39]. This study employed the use of *Cupriavidus metallidurans* CH34: an aerobic, gram-negative, facultative chemolithoautotrophic, rod-shaped *β-Proteobacterium* known for being resistant to the toxic effects of a number of metallic cations, e.g., Cu, Pb, Zn, Cd, Ag and Au [9,14,41–43]. Resistance is primarily facilitated by metal transporting ATPase efflux proteins in the cell envelope and cation reduction mechanisms in the cytoplasm, which have been shown to confer metal immobilisation [6,9,44]. This bacterium, which forms biofilms, was found to be living on the surface of gold grains obtained from auriferous soils in southern and northern Australia, and was shown to be able to precipitate aqueous gold-chloride species Reith et al. [14,15]. In addition, *C. metallidurans* strains were also present in biofilms on the surfaces of Brazilian platinum grains [25]. Therefore, a study of its interaction with aqueous platinum-chloride species found in natural systems should demonstrate comparable reactivity towards platinum.

2. Materials and Methods

2.1. Culturing of Cupriavidus metallidurans

Cupriavidus metallidurans strain CH34 (ATCC®43123, acquired from the American Type Culture Collection in Manassas, VA, USA) was grown in an ATCC® prescribed liquid medium containing 5 g/L peptone and 3 g/L beef extract (Difco Laboratories, Detroit, MI, USA). Before experimentation, the culture was transferred (~10% [vol./vol.] of inoculum at late stationary phase) to 13 mm × 100 mm borosilicate disposable culture test tubes (capped with plastic push caps to allow for free gas exchange and to prevent evaporation and contamination) and grown to early stationary growth phase (5 days) to maximize the amount of metabolically active biomass. These axenic batch cultures were incubated at room temperature (21–23 °C) under ambient atmospheric conditions.

After incubation, separate batches were pooled into 50 mL centrifuge tubes and homogenized (VWR Analog Vortex Mixer, VWR International, West Chester, PA, USA) to ensure a consistent cell density. For the platinum immobilisation experiments, 1 mL aliquots of the bacterial suspension were transferred to micro-centrifuge tubes and harvested by centrifugation at 12,000× *g* for 5 min using a VWR Galaxy 16 micro-centrifuge (VWR International, West Chester, PA, USA). After centrifugation, the supernatant was decanted and the cells were washed once by re-suspension into filter-sterilized distilled, deionized (DDI) water to remove any remaining culture medium. After vortexing, the bacterial suspension was centrifuged again at 12,000× *g* for 5 min. The supernatant was discarded and bacterial pellets were re-suspended into the experimental platinum solutions. The total number of bacteria in a washed sample was determined by direct counting using a Petroff–Hauser counting chamber and a phase contrast light microscope (Fluorescent Z1 microscope, Zeiss, Oberkochen, Germany).

2.2. C. metallidurans and Aqueous Platinum Experiments

The bacterial experiments were conducted to examine the role of inactive but viable *C. metallidurans* in the bio-immobilisation of platinum from aqueous solutions of platinum (II)-chloride (K_2PtCl_4, Premion®, 99.99+% [metal basis], Pt 46.4% minimum, Alfa Aesar®, Ward Hill, MA, USA) and platinum (IV)-chloride ($PtCl_4$, Premion®, 99.99+% [metal basis], Pt 57% minimum, Alfa Aesar®). Platinum salts were dissolved in DDI water at 16.2 MΩ/cm.

Washed *C. metallidurans* cell pellets (from 1 mL culture) were re-suspended in 1 mL aqueous platinum solutions (from stock solutions of 0.5 μM, 5 μM, 50 μM, 500 μM and 5000 μM final Pt(II) or Pt(IV) concentrations) at room temperature (21–23 °C) for 1 min, 1 h, 1 day, 2 weeks and 4 weeks. Experiments were maintained in the dark because platinum in solution is unstable when exposed to light [38]. Micro-centrifuge tubes containing the bacteria-platinum mixture were only removed from darkness to be vortexed weekly during the longer exposure times. All experiments were performed in triplicate.

Following exposure, reaction tubes were centrifuged at 12,000× *g* for 5 min and the supernatant was recovered for chemical analyses of residual, soluble platinum. The remaining bacterial pellets were washed one time by re-suspension in filter-sterilized DDI water to remove any unreacted aqueous platinum and centrifuged again at 12,000× *g* for 5 min. The wash solution was decanted and the reacted culture was re-suspended in 1 mL of filter-sterilized DDI water in preparation for whole mount transmission electron microscopy or for the examination of bacterial viability. Bacterial pellets were fixed using 1 mL of 2 wt % glutaraldehyde for ultra-thin section transmission electron microscopy (described below).

2.3. C. metallidurans—Aqueous Pt(II)- and Pt(IV)-Chloride Dose–Response Experiments

The effect of aqueous Pt(II)- and Pt(IV)-$chloride_{(aq)}$ on bacteria viability was determined using the spread plate method [45]. Briefly, reacted cells were washed and re-suspended in 1 mL of DDI water and used in a serial dilution series with filter-sterilized DDI water. Each dilution was plated

in duplicate on peptone–beef extract–agar plates that contained (in g/L) peptone, 5; beef extract, 3; and agar, 15 (Difco Laboratories). Plates were incubated for four days at room temperature (21–23 °C) under ambient atmospheric conditions. Colony-forming units (cfu) were counted with the aid of a New Brunswick C-110 Colony Counter with digital counter and probe.

2.4. Chemical Analyses of Solutions and Quantification of Pt Associated with Cells

Platinum concentrations were measured over the course of the experiments using a Perkin–Elmer Optima-3000 DV system inductively coupled plasma atomic emission spectrometer (ICP-AES, ICP-AES; Shelton, CT, USA). Instrumental uncertainty for measured platinum was <5%, with a detection limit of 0.05 μM. Samples for ICP-AES were diluted as necessary (1:10 or 1:100 vol./vol.) with filter-sterilized DDI water directly prior to analyses. Platinum standards for calibration were prepared with aqueous Pt(II) and Pt(IV) stock solutions used in the laboratory-based *C. metallidurans* and aqueous platinum experiments. The pH of the stock solutions was measured using a Denver Instrument basic pH meter (Bohemia, NY, USA). The electrodes were calibrated in buffer solutions of pH 4, 7 and 10. Analytical uncertainty of pH measurements is ±0.01 units. The pH of the platinum solutions after exposure to bacteria was compared to the pH of stock solutions using ColorpHast® non-bleeding indicator strips (Merck, Etobicoke, ON, Canada).

In order to calculate the effective concentration of immobilised platinum within the bacterial cells, the amount of soluble platinum remaining in solution after reacting with *C. metallidurans* was quantified by ICP-AES. These results were then subtracted from the known starting concentrations of soluble platinum (i.e., the stock aqueous platinum solutions) reacted with the bacteria, and normalized to the volume of 1 billion *C. metallidurans* cells to determine the concentration of platinum inside the cells. The volume calculation for *C. metallidurans* was based on diameter and length measurements of bacteria shown in the accompanying whole-mount TEM micrographs (Figures 1–3, 5 and 6), modeled as a cylinder bounded by two half spheres (see Equation (1), [46]):

$$V = 4/3(\pi r^3) + \pi r^2 h \quad (1)$$

2.5. Transmission Electron Microscopy (TEM)

Unstained whole sample mounts and thin sections of T = 0 control (prior to reaction with the Pt solutions) and Pt-reacted *C. metallidurans* were examined using a Phillips CM-10 transmission electron microscope (TEM; FEI, Hillsboro, OR, USA) operated at 80 kV (60 kV for ultra-thin sections). The whole mounts were prepared by floating Electron Microscopy Sciences (EMS; Hatfield, PA, USA) Formvar carbon-coated 100-mesh copper grids on a drop of culture for several minutes to allow the bacteria to adsorb to the grid. Grids were then washed to remove salts by gentle dipping into a drop of filter-sterilized DDI water. The grids were allowed to air-dry prior to microscopy.

Samples for ultra-thin sectioning were fixed overnight at room temperature in $2\%_{(aq)}$ glutaraldehyde (EMS). Fixed cultures were subsequently centrifuged at 14,000× *g* for 1 min. The supernatant was discarded and the remaining bacterial pellet was enrobed in 2% (weight/volume) Noble agar (Difco Laboratories) and dehydrated using a 25%, 50% 75% and three × 100% acetone series (incubations were 15 min each). The acetone was slowly replaced with an EMS epoxy resin (the enrobed culture was incubated at 1 h intervals in a 1:1 [*v*/*v*], 1:3 [*v*/*v*] and 1:9 [*v*/*v*] acetone:epoxy resin series). Epoxy resin contained a 2.5:2:1 volume ratio of Embed 812, DDSA (dodecenyl succinic anhydride) and NMA (nadic methyl anhydride). Samples were incubated overnight in 100% epoxy resin and then transferred to moulds with fresh epoxy resin containing the accelerator DMP-30 (2,4,6-tri(dimethylaminoethyl)phenol, EMS). Ratios by volume were 2.5:2:1:0.15. The molds were cured in a 60 °C oven (Blue M Electric Company Bacteriological Incubator, Watertown, WI, USA) for 48 h, until hard. Embedded samples were ultra-thin sectioned using a Reichert-Jung Ultracut E ultramicrotome (Vienna, Austria) equipped with a Diatome™ diamond knife to a thickness of 70 nm and collected on Formvar carbon-coated 100-mesh copper grids.

2.6. X-ray Absorption Spectroscopy (XAS) Data Collection

X-ray Absorption Spectroscopy energy measurements from the bacteria-platinum reactions, including XANES (X-ray absorption near edge structure) and EXAFS (extended X-ray absorption fine structure), were conducted at the Pacific Northwest Consortium/X-ray Science division (PNC-XSD) sector 20-BM beamline at the Advanced Photon Source, Argonne National Laboratory, Argonne, IL, USA. The oxidation state of platinum can be determined by XANES while information regarding the binding partners and local coordination of platinum is provided by EXAFS data. Determining the oxidation state and binding partners of platinum will shed light on how aqueous platinum binds to bacterial cells [38]. X-ray Absorption Spectroscopy energy measurements of the Pt-L_3 edge were collected from each sample and were calibrated to the inflection of the Pt foil edge at 11,564 eV [47].

For the XAS measurements, *C. metallidurans* cells were reacted as described above. For XAS, replicate reactions were harvested by centrifugation, i.e., cells were pelleted, and re-suspended in 200 µL water in order to concentrate the sample for better chemical detection. The reacted bacterial samples were then placed in an acid-resistant Teflon fluid cell with Teflon-coated Kapton film (Dupont®, Wilmington, NC, USA) windows or were pipetted directly onto Whatman® 42 Ashless Filter Papers (Maidston, UK). XAS measurements on the bacterial samples were conducted in fluorescence mode.

Reference compounds were needed to determine the chemical state of bound platinum in these reactions. Standards were selected on the criteria that they represent the most likely oxidation states and bonding partners of platinum expected in the reacted, bacterial samples. The XAS spectra for model compounds including platinum (IV)-chloride ($PtCl_4$), platinum (IV)-cyanide ($K_2Pt(CN)_6$), platinum (II)-chloride (K_2PtCl_4), platinum (II)-cyanide ($K_2Pt(CN)_4$) and platinum (II)-tetraamine nitrate ($(NH_3)_4Pt(NO_3)_2$) were measured in aqueous solution in transmission mode. Liquid stocks (up to 65 mM) were prepared from solid compounds without pH adjustment. XAS spectra for platinum (IV)-oxide hydrate ($PtO_2 \cdot xH_2O$), platinum (II)-cis-diamminedichloride (cisplatin, $Pt(NH_3)_2Cl_2$), platinum (II)-sulphide (PtS) and platinum foil (Pt) were measured in solid form in transmission mode due to their insoluble nature. With the exception of the foil and platinum (II)-sulphide, the standards were placed in teflon fluid cells with kapton film windows. Platinum (II)-sulphide was a precipitate and was concentrated onto MF-Millipore™ 0.45 µm, 13 mm membrane filters (Burlington, NJ, USA). Model compounds were commercially acquired from Alfa Aesar® and Sigma-Aldrich® (with exception of platinum (II)-sulphide, which was synthesized in the laboratory by mixing equal molar solutions of aqueous platinum (II)-chloride (K_2PtCl_4) with aqueous sodium sulphide 9-hydrate [$Na_2S \cdot 9H_2O$] (J.T. Baker®, Phillipsburg, NJ, USA) to produce a black (PtS) precipitate (confirmed by Energy Dispersive Spectroscopy). The reference spectrum of the platinum foil was simultaneously collected during measurement of all standards and reacted, bacteria samples. Incident energy from the beam did not alter the chemistry of the standards or samples.

2.7. XAS Data Analysis

ATHENA analysis software was used to process XAS data [48]. Energy scans from samples and standards were calibrated and aligned to the standard platinum foil reference energy. Multiple scans were collected for each sample and were averaged to produce a single spectrum representative of platinum's oxidation and complexation state in that sample. XANES spectra were then analysed by comparing the energy position of the platinum edge in the reacted, bacteria samples to the energy edge location from the standards. Linear combination fitting in ATHENA mathematically identified which standard(s) aligned with the energy edge of the immobilized platinum. Energy position alignment corresponded to the oxidation state of the immobilized platinum [38]. EXAFS data analysis was performed in ARTEMIS, a XAS analysis software program complimentary to ATHENA [48]. Mathematical derivatives of post edge energy peaks from the bound platinum in the bacterial samples were fitted to post edge energy peaks from the platinum in the standards. Peak alignment, normalized to platinum chloride standards, indicated potential binding partners of the immobilized platinum [38].

3. Results

3.1. Laboratory-Based C. metallidurans and Aqueous Platinum Experiments

The addition of K_2PtCl_4 and $PtCl_4$ to filter-sterilised, DDI water promoted the hydrolysis of water, as indicated by a drop in the pH of the overall solution. The pH of the K_2PtCl_4 solutions were 5000 μM (pH 4.2), 500 μM (pH 5.2), 50 μM (pH 5.8) and 5 μM (pH 6.1). The pH of the $PtCl_4$ solutions were 5000 μM (pH 2.1), 500 μM (pH 3.0), 50 μM (pH 4.1) and 5 μM (pH 5.3). The pH of the platinum solution after reaction with bacteria did not change significantly from the pH of the stock solution. The addition of 5000 μM K_2PtCl_4 turned the pellet a brown-grey color in all exposure times. Similarly, the addition of 5000 μM $PtCl_4$ to the washed bacterial pellet immediately turned from white to yellow at all exposure times. Pellet color changes were much fainter or not identifiable at lower concentrations. Color changes provide macroscopic evidence that platinum was immobilized from solution, i.e., bound to cell surfaces (staining), or immobilized within the cells.

Tables 1 and 2 were prepared by comparing cfu counts of the Pt-reaction systems to the unreacted count for the appropriate exposure times. Results were normalized to a standard cfu count (5.0×10^8 cfu/mL) to allow comparison between exposure times and treatments. The experiments demonstrated that cell death was 'instantaneous' upon exposure of bacteria to 5000 μM Pt(II) and Pt(IV), i.e., no colonies grew. Platinum toxicity was directly proportional to concentration and exposure time, with Pt(II) solutions being slightly less toxic than Pt(IV) solutions for a given particular concentration, exhibiting a minimum inhibitory concentration between 0.5 to 5 μM versus 0.5 μM, respectively. Control experiments demonstrated that osmotic and/or pH effects were not responsible for the reduction in cell counts (data not shown).

Table 1. Toxicity study where *C. metallidurans* was reacted with aqueous Pt(II).

[Pt(II)]	cfu/mL after 1 min Exposure	cfu/mL after 1 h Exposure	cfu/mL after 1 day Exposure
0 μM	$5.0 \pm 0.2 \times 10^8$	$5.0 \pm 0.2 \times 10^8$	$5.0 \pm 0.2 \times 10^8$
0.5 μM	$4.9 \pm 0.1 \times 10^8$	$2.7 \pm 0.1 \times 10^8$	$4.6 \pm 0.1 \times 10^8$
5 μM	$3.7 \pm 0.2 \times 10^8$	$3.2 \pm 0.2 \times 10^8$	$4.3 \pm 0.2 \times 10^6$
50 μM	$4.1 \pm 0.3 \times 10^8$	$1.3 \pm 0.1 \times 10^7$	$2.1 \pm 0.1 \times 10^3$
500 μM	$9.9 \pm 0.3 \times 10^6$	0	0
5000 μM	0	0	0

Table 2. Toxicity study where *C. metallidurans* was reacted with aqueous Pt(IV).

[Pt(IV)]	cfu/mL after 1 min Exposure	cfu/mL after 1 h Exposure	cfu/mL after 1 day Exposure
0 μM	$5.0 \pm 0.2 \times 10^8$	$5.0 \pm 0.2 \times 10^8$	$5.0 \pm 0.2 \times 10^8$
0.5 μM	$4.5 \pm 0.1 \times 10^8$	$3.2 \pm 0.1 \times 10^8$	$3.3 \pm 0.1 \times 10^8$
5 μM	$4.9 \pm 0.3 \times 10^8$	$2.5 \pm 0.1 \times 10^8$	$7.6 \pm 0.4 \times 10^7$
50 μM	$1.1 \pm 0.1 \times 10^8$	$6.4 \pm 0.4 \times 10^6$	$4.8 \pm 0.3 \times 10^3$
500 μM	$6.6 \pm 0.4 \times 10^2$	0	0
5000 μM	0	0	0

ICP-AES results are shown in Tables 3 and 4. Immobilization began immediately upon exposure to platinum. As exposure time increased for a particular concentration, the amount immobilized also increased, however, the immobilization rate at these longer exposure times did not match the rate immobilized at 1 min. The effective concentration of platinum associated with the bacteria, based on cell volume, exceeded the T = 0 solution concentrations in all reaction systems demonstrating uptake by *C. metallidurans*. Cell saturation was not reached except after 1-day exposure time for bacteria in 5000 μM Pt(II) solutions.

Table 3. Immobilisation study where *C. metallidurans* was reacted with aqueous Pt(II).

[Pt(II)]	Intracellular Concentration after 1 min Exposure (mM)	Intracellular Concentration after 1 h Exposure (mM)	Intracellular Concentration after 1 day Exposure (mM)
5 μM	1.8 ± 0.01	1.6 ± 0.02	15 ± 0.3
50 μM	51 ± 0.3	44 ± 0.5	67 ± 1
500 μM	120 ± 0.70	120 ± 1.5	410 ± 7.3
5000 μM	850 ± 12	800 ± 12	850 ± 6.5

Table 4. Immobilisation study where *C. metallidurans* was reacted with aqueous Pt(IV).

[Pt(IV)]	Intracellular Concentration after 1 min Exposure (mM)	Intracellular Concentration after 1 h Exposure (mM)	Intracellular Concentration after 1 day Exposure (mM)
5 μM	1.6 ± 0.01	2.6 ± 0.02	9.6 ± 0.05
50 μM	11 ± 0.05	13 ± 0.1	40 ± 0.2
500 μM	45 ± 0.22	160 ± 1.3	210 ± 1.2
5000 μM	310 ± 5.8	350 ± 0.45	870 ± 0.75

3.2. Transmission Electron Microscopy (TEM)

Micrographs of the control (unreacted bacteria) are shown in Figure 1. TEM micrographs of *C. metallidurans* exposed to platinum solutions are presented in Figures 2–6. Note, the cytoplasmic contents are clearly visible in Figure 1A compared to the lack of internal detail of the cell in the ultra-thin section shown in Figure 1B. The cell envelope in the control image is visible as a white "halo" around the cell, i.e., it is less dense than the plastic. As no metal staining was applied to these bacteria, any increase in electron density in bacteria from the Pt-reacted systems are attributed to the immobilisation of aqueous platinum.

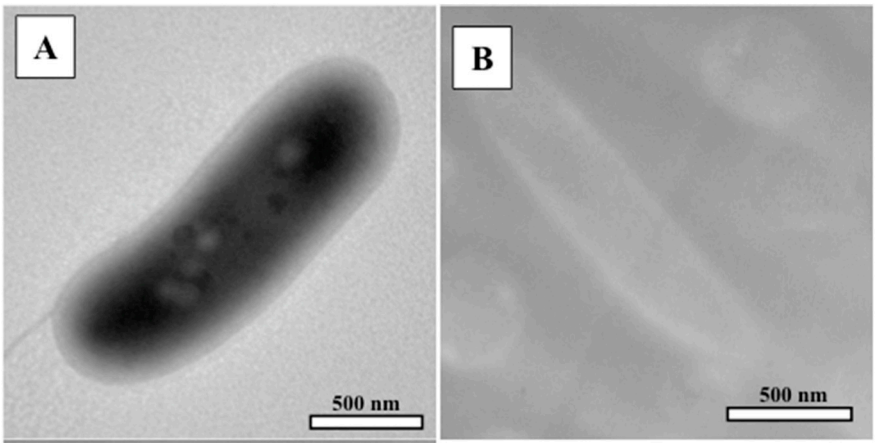

Figure 1. (**A**) Whole mount TEM micrograph of an unreacted *C. metallidurans* cells. Note, the cell envelope is generally electron transparent; (**B**) Unstained, ultra-thin section TEM micrograph of unreacted *C. metallidurans*. Note the internal detail of cell is lacking because no stain was applied.

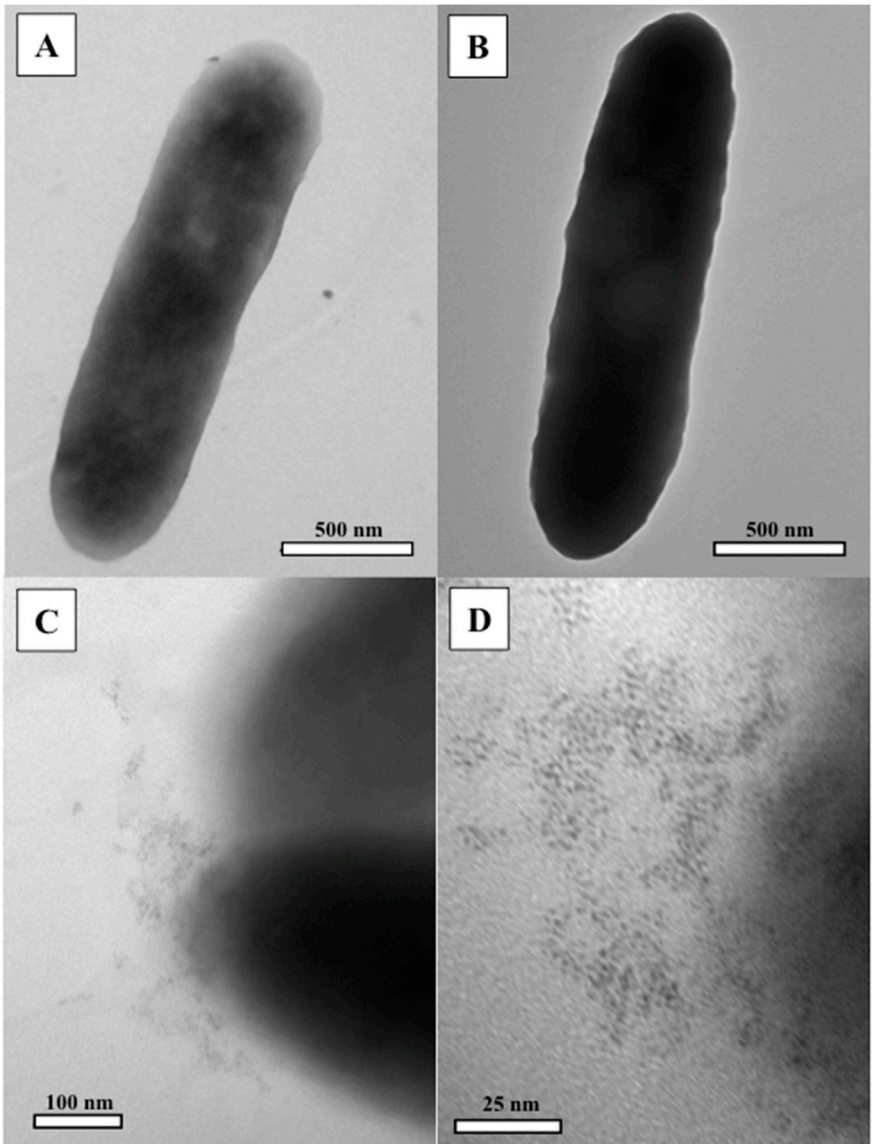

Figure 2. Whole mount TEM micrographs of *C. metallidurans* reacted with 500 μM Pt(II) for: (**A**) 1 min; (**B**,**C**) 1 day. (**D**) Micrograph of nanoparticles in Figure 2C. At 1 day, all cells were stained (**B**) but only some cells had produced nanoparticles (**C**,**D**).

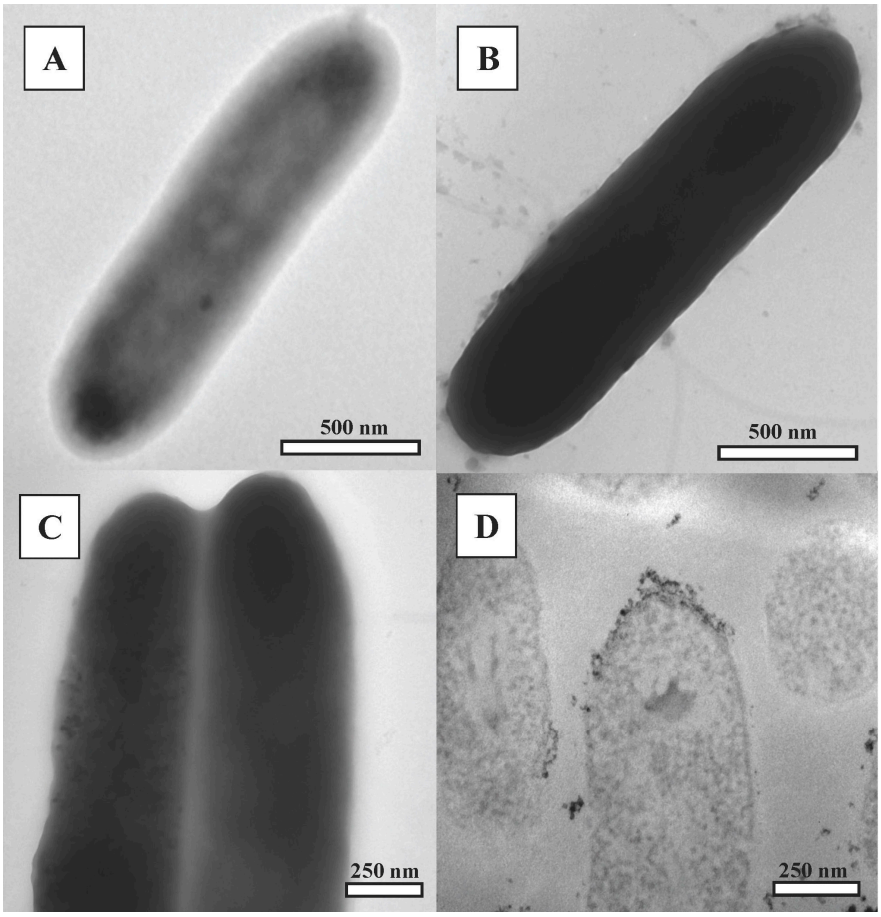

Figure 3. Whole mount TEM micrographs of *C. metallidurans* exposed to 5000 μM Pt(II) for: (**A**) 1 min, binding of Pt is minimal as cell remains generally electron transparent; (**B**) 1 h; and (**C**) 1 day. At longer incubation times (**B**,**C**), cell staining is apparent in all cells; (**D**) Ultra-thin section TEM micrograph of *C. metallidurans* exposed to 5000 μM Pt(II) for 1 h. Nanoparticle Pt is immobilized along the cell envelope, in particular at some cell poles, and in the cytoplasm.

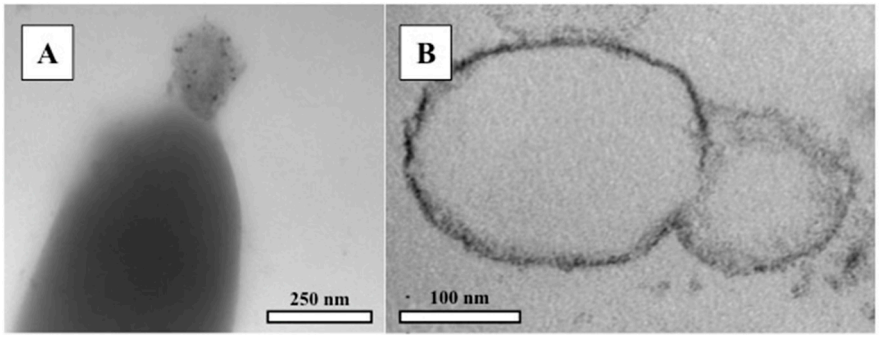

Figure 4. (**A**) Whole mount TEM micrograph of immobilized Pt along an outer membrane vesicle blebbing off of the cell envelope (1 h exposure at 5000 μM Pt(II)); (**B**) Ultra-thin section TEM micrograph of Pt immobilisation along the periphery of an outer membrane vesicle (1 h exposure at 5000 μM Pt(II)).

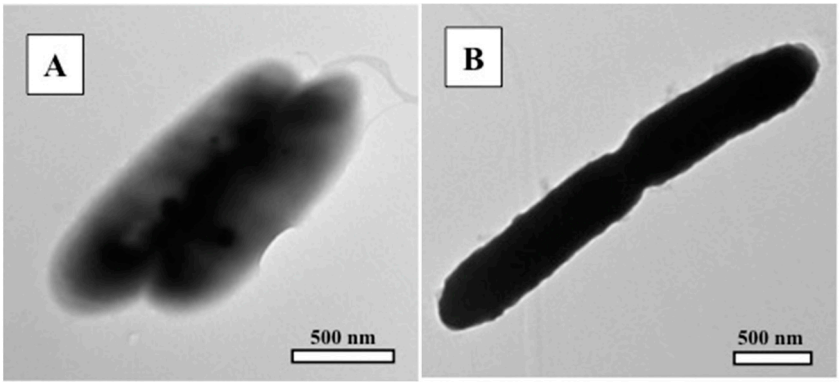

Figure 5. Whole mount TEM micrographs of *C. metallidurans* reacted with 500 μM Pt(IV) for: (**A**) 1 min, and (**B**) 1 day. As incubation time increased, Pt staining became more pronounced. Colloidal platinum was not observed at any exposure time.

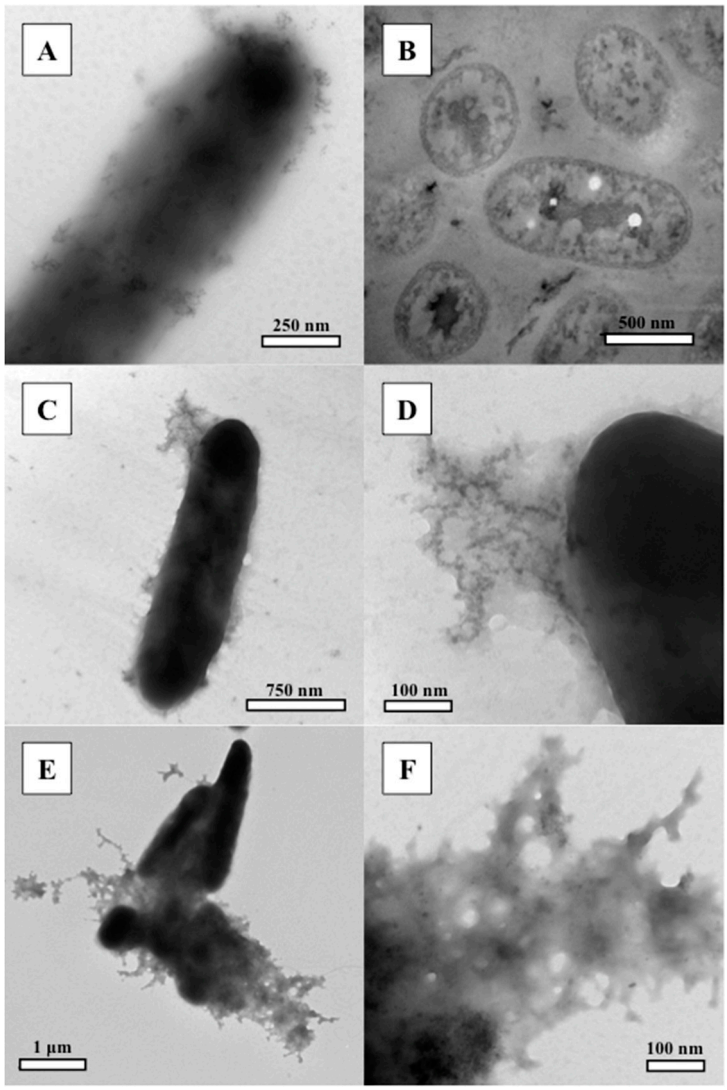

Figure 6. TEM micrographs of *C. metallidurans* reacted with 5000 μM Pt(IV) for: (**A**) 1 min (whole mount); (**B**) 1 h (ultra-thin section). Pt has been immobilized at the cell envelope and within the cell; (**C**,**D**) 1 h (whole mount); (**E**,**F**) 1 day (whole mount). Cells in (**C**–**F)** have lysed and cytoplasmic material possesses colloidal Pt. Staining of cells becomes more pronounced at longer incubation times (**C**–**F**).

Figure 2A demonstrates that bacterial staining occurs immediately upon exposure to 500 μM Pt(II), however, not all bacteria at 1 min and 1 h were stained by platinum. Generally, longer exposure times revealed darker staining (Figure 2B). Some bacteria produced nanometre-scale platinum colloids at 1 day (Figure 2C,D). Nanoparticles were not observed at shorter exposure times. Figure 3A shows that, at 1 min, some bacterial cells did not bind platinum from the 5000 μM Pt(II) solution. The majority of cells were stained with platinum at this exposure time point and at 1 h (Figure 3B). All bacteria were observed to be considerably darker after 24 h (Figure 3C). Platinum colloid formation began at 1 h and 1 day exposure times (Figure 3C). An ultra-thin section TEM micrograph of a bacteria exposed to 5000 μM Pt(II) for 1 h is shown in Figure 3D. Platinum nanoparticles appear along the periphery of the cell envelope and within the cytoplasm. Figure 4A shows a partially lysed bacterium (a bacterium that has split open), with platinum nanoparticles bound in cytoplasmic material. Cell lysis could be a response to platinum toxicity. In Figure 4B, Pt-binding into the outer membrane (OM) appears to have caused a physical disruption to the OM packing order, resulting in vesicle formation. Shedding OM vesicles, as a consequence of membrane rearrangement to accommodate the Pt ions, has the benefit of keeping toxic material away from the cell [9,38]. These vesicles were important sites of Pt immobilisation.

As indicated by the micrographs in Figures 5 and 6, *C. metallidurans* responded to Pt(IV) solution much like it did to Pt(II) solutions. Cell staining appeared to be immediate but not complete at 1 min (Figure 5A). Longer exposure times produced a darker stain (Figure 5B). Similarly, nanoparticles were observed to precipitate along the cell envelope and within the cell (Figure 6A,B). Cell lysis was observed at 5000 μM Pt(IV). Released cytoplasmic material bound platinum nanoparticles (Figure 6C–F). As with 5000 μM Pt(II) solutions, cell lysis could have been a response to platinum-chloride itself, the low pH of the solution, or a combination of both.

It was noted that cells adhered to each other upon exposure to platinum solutions, perhaps as a result of the neutralization of anionic charge groups on the cell envelope by platinum and hydronium, allowing ionic interactions or hydrophobicity to cause cellular aggregation [49]. This response could protect some cells at the interior by shielding them from the platinum complexes. This may also explain why immediate platinum binding was not observed by all cells.

3.3. Synchrotron X-ray Absorption Spectrosocpy (XAS)

XAS spectra in Figure 7 show the speciation and binding partners of the platinum immobilized by *C. metallidurans* CH34. Figure 7A is the XANES spectra of bacteria reacted with 5000 μM Pt(II) and Pt(IV) for up to 4 weeks. The peak edge binding energy of Pt(II) is slightly less than the Pt(IV) peak, indicating that electrons are bound more tightly in the more oxidized platinum species. There is no decrease in binding energy for either immobilized platinum species, indicating that synchrotron radiation did not detect a change in platinum oxidation over the course of the experiments. It is important to note that at least 10 wt % of the immobilized platinum must be reduced before synchrotron radiation can detect the change in speciation. The spectra in Figure 7A are representative of the XANES spectra obtained at lower concentrations (data not shown).

Figure 7B shows the XANES and EXAFS spectra of bacteria reacted with 5000 μM (1000 μg/mL) Pt(II) for 4 weeks. Similar spectra were obtained for reactions with 5000 μM (1000 μg/mL) Pt(IV), as well as with 500 μM Pt(II) and Pt(IV) solutions (data not shown). Examination of the EXAFS region in Figure 7B demonstrated that the Pt-Cl "fingerprint" decreased in intensity over time, suggesting that the chlorine bound to Pt(II) was replaced by another binding partner. Figure 7C indicates that the replacement was 'immediate', as the shortening of radial distance between bonds occurred within 1 min, however, gradual immobilization of additional Pt(II) with substitution of chlorine continued over the 4-week experiment. The ligand replacing chlorine is best matched to oxygen on a carboxyl group, as the radial distance indicative of a Pt–O bond on carboxyl groups is ~2.06 Å, which compared closely to our 2.07 Å and 2.08 Å bond distances [50–52].

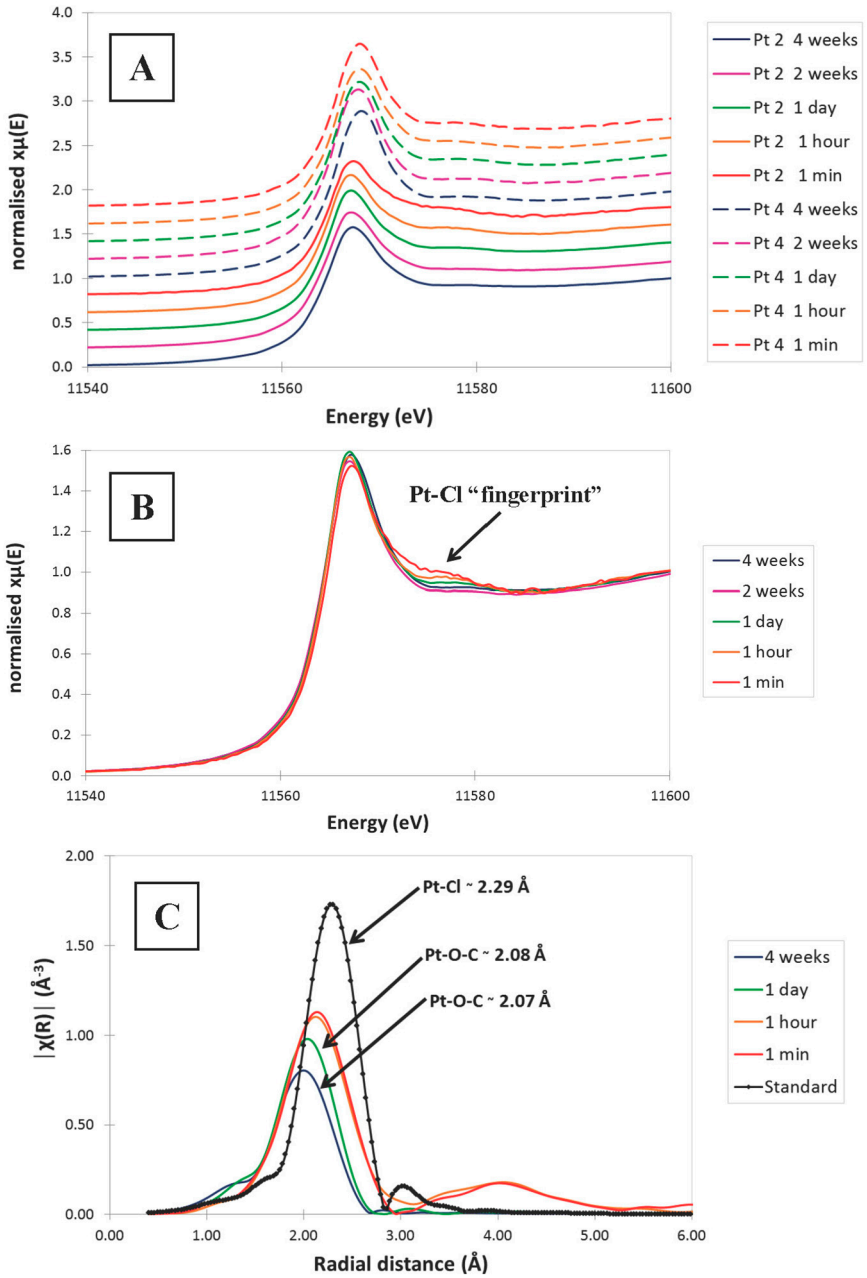

Figure 7. (**A**) XANES spectra of bacteria reacted with 5000 μM Pt(II) and Pt(IV) solutions for up to 28 days. Note that the edge peaks of Pt(IV) are slightly higher in energy than the Pt(II) peaks due to the higher oxidation state. There is no downward shift in peak energy for either the Pt(II) or Pt(IV) over the 28 days, indicating that synchrotron energy did not detect any reduction of platinum; (**B**) XANES and EXAFS spectra of bacteria reacted with 5000 μM Pt(II) solutions for up to 28 days. The arrow notes the Pt-Cl "fingerprint", which decreases over time. There is no downward shift in peak energy for Pt(II) over the 28 days, indicating that synchrotron energy did not detect any reduction of platinum; (**C**) EXAFS spectra of bacteria reacted with 5000 μM Pt(II) solutions for up to 28 days. The solid arrows show the first shell-binding partners of Pt. Note that Pt-Cl bonding shifts to Pt-O-C over time.

4. Discussion

The interaction of *C. metallidurans* with $PtCl_{4(aq)}$ and $K_2PtCl_{4(aq)}$ resulted in a variety of bacterial responses: cell death and cytolysis, platinum immobilisation as well as nanoparticle formation. The degree of each response was directly proportional to platinum concentration and time (Tables 1–4).

The literature lacks consistent experimental data on Pt(II) and Pt(IV) complexation. Potential Pt(II) complexes present in the reactions systems included Pt(II), $Pt(OH)_n^{-2+n}$ and $PtCl_n^{-2+n}$. Likely Pt(IV) compounds included Pt(IV), $Pt(OH)_n^{-4+n}$ and $PtCl_n^{-4+n}$, but very little data exists for these species [29,30,34,37,53]. EXAFS confirmed platinum-chloride to be the dominant aqueous species prior to reaction with bacteria. The observed uptake of these Pt(II) and Pt(IV) complexes from solution is consistent with the literature-described uptake of other metals by bacteria i.e., immobilisation occurs primarily within the cell envelope and within the cytoplasm [6,54].

Platinum staining occurred evenly throughout the cell and nanoparticle formation and immobilisation occurred intracellularly, at the cell surface and extracellularly, comparable to that observed by Konishi et al. [39]. Cell surface reactivity is controlled by the proton exchange capacity of carboxyl (R-COOH), phosphoryl (R-OPO_3H_2 and $(RO)_2$-$P(OH)_2$), amine (R-NH_3^+) and hydroxyl (R-OH) functional groups in the cell envelope. In all but the 500 µM and 5000 µM Pt^{4+} reactions, most carboxyl groups would have been deprotonated, i.e., negatively charged and available for reaction with oxidised platinum. In contrast, phosphoryl, amine and hydroxyl groups would have remained mostly protonated and positively charged at the pH conditions consistent with the acidity of aqueous platinum solutions used in this experiment [54–56]. XANES and EXAFS spectra clearly show the replacement of chlorine for oxygen on carboxyl groups to be the most likely binding mechanism. It is worth noting that the immobilised platinum occurred as platinum-organo complexes at the cell surface, suggesting that organo-platinum complexes may be preferred to inorganic complexes when bacteria are present. This process has been described in natural systems where carboxyl functional groups on soluble organic acids are able to react with platinum to form stable platinum-organo complexes [32,36,53,57].

As suggested by Beveridge and Murray [54], metal (platinum) binding to the cell envelope likely proceeded first as a stoichiometric event where reactive sites bound platinum and then as a nucleation event, where nanoparticles grew by accretion in a non-stoichiometric fashion, which continued at a slower pace, when it occurred at all. The rapid uptake of platinum may have occurred because membrane transporter proteins were unable to regulate the entry of these particular compounds, i.e., all complexes freely entered the cell driven by the chemiosmotic gradient that existed across the cell envelope [6]. Passive diffusion would have ceased nearly instantaneously once platinum concentrations within the cell equalled the platinum concentration within the solutions. Aqueous platinum that entered the circumneutral pH of the cytoplasm presumably bound to deprotonated functional groups and complexed with carboxyl functional groups [55,56] shifting the equilibrium towards continued uptake of Pt.

Bacterial cells that remained viable following exposure to low concentrations of platinum would have presumably initiated a biological response to mitigate toxicity in an attempt to survive. Under limiting carbon conditions, represented by early stationary phase culture conditions, CH34 will degrade short-chain fatty acids, dicarboxylated compounds, or energy-storage products, such as polyhydroxybutyrate (PHB) [58]. Internalized metals inhibit the function of important enzymes, bind to important functional groups, and out-compete other important physiological cations. Detoxification responses include chemical reduction [39] or complexation of the metal to a less toxic state and/or efflux of the metal to the outside of the cell. These mitigation responses drain the cell of energy and cause an oxidative stress, leading to continued cell death at longer exposure times [6,7]. Although XANES did not indicate platinum reduction, the appearance of dark, electron dense nanometre-scale platinum colloids in the cytoplasm (and at the cell envelope) is evidence that some platinum reduction occurred [39].

The relationship between toxicity and immobilization emerges from a comparison of Table 1 vs. Tables 2 and 3 vs. Table 4. For a particular platinum species, immobilization of platinum is generally correlated with the concomitant death of cells, e.g., the more platinum that was immobilized, the more cells that died. Resistance of *C. metallidurans* to pH 4.1, 50 µM Pt(IV) solution demonstrates that the toxicity experienced by the cells in the 5000 µM Pt(II) solution (pH 4.2) was primarily due to a platinum effect versus a pH effect. Similarly, cell death was 'immediate' in 500 µM and 5000 µM Pt^{4+}

solutions, but when *C. metallidurans* was exposed to pH comparable solutions of HCl, corresponding levels of cell death were not observed (data not shown). Intuitively, acidic solutions will induce some cell death; however, these results demonstrate that platinum immobilization triggered most of the observed toxicity. It is important to note that dead cells cannot 'actively' bind platinum, yet immobilization occurred long after cell death, e.g., the 5000 μM Pt(IV) solution killed all bacteria within 1 min and platinum immobilization continued at least 1 day in this reaction system. Dead cells no longer metabolise and the proton motive force that effluxes protons to the cell surface does not operate, consequently, there is less competition for platinum to bind to anionic carboxyl groups [59]. The ionic adsorption of cations to dead *C. metallidurans* cells is known to be higher than the reactivity of live cells [41]. In this situation, the appearance of new reactive sites from denatured cell membranes and lysed cytoplasmic contents likely contributed to the continued immobilisation of platinum, even when cell death was 'instantaneous'.

Further comparison of Tables 1 and 2 reveals two important differences between the Pt(II) reaction systems and Pt(IV) reaction systems. Firstly, Pt(II) reactions were slightly less toxic than Pt(IV). While Pt(II)chloride solutions were not as acidic as Pt(IV)chloride solutions, bacteria that remained viable following exposure may have been able to neutralize and pump out Pt(II) cations easier than Pt(IV) cations via *C. metallidurans*'s divalent cation efflux ATPases [44]. Intuitively, in a low metabolic state, i.e., brought about by being re-suspended in water, if the bacteria could not efflux the highly oxidized platinum, then the cell's attempt to neutralise it internally could have been brought about by a fatal oxidative stress [6,15]. The minimum inhibitory concentrations measured in this experiment were one to two orders of magnitude less than that measured by Etschmann et al. [60], i.e., 0.5 to 5 μM (Table 1) versus 200 μM for Pt(II)-chloride and 0.5 μM (Table 2) versus 17.5 μM for Pt(IV)-chloride. This discrepancy is explained by the affinity of Pt(II) and Pt(IV) for carboxyl groups (Figure 7) and by the use of a ca. 10 mM gluconate culture medium in the Etschmann et al. [60] MIC experiment; the gluconate would have complexed the Pt, reducing toxicity. It is also important to note that the bacteria were also able to immobilize more platinum from Pt(II) solutions than from Pt(IV) solutions. From a concentration and charge character of platinum vs. hydronium perspective, platinum exceeded hydronium in the Pt(II) system by approximately two orders of magnitude and generally balanced the hydronium concentration in the Pt(IV) systems. Therefore, Pt(II) would have easily out-competed hydronium for carboxyl binding sites whereas Pt(IV) would have had more competition and therefore less opportunity to be bound and immobilised.

Therefore, we believe that platinum and gold share quite similar chemical characteristics, and that a Pt detoxification pathway remains to be discovered. It is not surprising that the reactions of *C. metallidurans* and platinum are similar to those that have been observed between *C. metallidurans* and gold. Reith et al. [15] demonstrated that *C. metallidurans* rapidly accumulates Au(III)-complexes from solution and forms intermediate Au complexes and Au^0 nano-precipitates. Likewise, platinum was readily immobilised by carboxylic functional groups on and in the bacteria, and as observed via TEM, nanometre-scale Pt nanoparticles were also formed, though diagenesis of Pt into nano-phase colloidal and crystalline materials was less active than for gold in *C. metallidurans*.

The traditional notion that platinum is inert has been challenged by a new biogeochemical paradigm [25,33] where the transport of platinum from the mantle to the crust and the subsequent abiotic weathering of Platinum Group Metal (PGM)-bearing host rocks represents an incomplete metallogeny of placer platinum deposits. Subsequent and reoccurring dissolution, transportation and precipitation of platinum by biological and abiotic processes, potentially over geologic time, [25,34,35,37,61] are now considered to be key components in placer PGM formation in tropical or sub-tropical climates. The biogeochemical examination of candidate platinum compounds in this study have demonstrated that there is still more to learn about the mobility of platinum in natural systems. Specifically, this work has highlighted the importance of nanophase- and organo-platinum compounds in platinum exploration, which could help define exploration targets for the mining industry.

5. Conclusions

While *Cupriavidus metallidurans* immobilized appreciable amounts of platinum, i.e., ca. molar intracellular concentrations (Tables 3 and 4), it did not transform the platinum into appreciable amounts of secondary platinum. TEM clearly demonstrated that platinum is immobilized within the cell envelope and cytoplasm, occurring primarily via chemical immobilization of aqueous platinum species on carboxyl groups. Although platinum reduction was not detected using synchrotron methods, the reduction of at least some of the oxidized platinum to 1–2 nm particles of elemental platinum was observed in a number of reaction systems. Due to the ubiquitous nature of bacteria in near-Earth surface environments and the high affinity of both Pt(II) and Pt(IV) for organically derived carboxyl functional groups, this study suggests that organo-platinum must be important in natural systems where platinum-bearing materials are exposed to weathering conditions, potentially leading to the dispersal of platinum in association with organic acids derived from the biosphere.

Acknowledgments: Electron Microscopy was performed in the Nanofabrication and Biotron Imaging facility (Western University, London, ON, Canada). Synchrotron analyses were conducted at the APS-PNC/XSD facilities at the Advanced Photon Source, supported by the US Department of Energy—Basic Energy Sciences, the Canadian Light Source and its funding partners, the University of Washington, and the Advanced Photon Source. Use of the Advanced Photon Source, an Office of Science User Facility operated for the U.S. Department of Energy (DOE) Office of Science by Argonne National Laboratory, was supported by the U.S. DOE under Contract No. DE-AC02-06CH11357. Funding was provided by an Australian Research Council Discovery Grant DP20106946 to Reith, and a Canadian NSERC Discovery Grant to Southam. We thank the two anonymous reviews for their contributions to the manuscript.

Author Contributions: G.C., F.R. and G.S. conceived and designed the experiments; G.C. performed the bacterial culture experiments and the electron microscopy; L.M., D.B. and R.A.G. guided the synchrotron measurements done by G.C. and G.S., and helped analyze and interpret the data; S.G.C. wrote the first draft of the paper (MSc thesis); G.S. prepared the manuscript for publication.

Conflicts of Interest: The authors declare no conflict of interest.

References

1. Enders, M.S.; Knickerbocker, C.; Titley, S.R.; Southam, G. The role of bacteria in the supergene environment of the Morenci Porphyry Copper Deposit, Greenlee County, Arizona. *Econ. Geol.* **2006**, *101*, 59–70. [CrossRef]
2. Reith, F.; Brugger, J.; Zammit, C.M.; Gregg, A.L.; Goldfarb, K.C.; Andersen, G.L.; Desantis, T.Z.; Piceno, Y.M.; Brodie, E.L.; Lu, Z.; et al. Influence of geogenic factors on microbial communities in metallogenic Australian soils. *ISME J.* **2012**, *6*, 2107–2118. [CrossRef] [PubMed]
3. Southam, G.; Saunders, J.A. The geomicrobiology of ore deposits. *Econ. Geol.* **2005**, *100*, 1067–1084. [CrossRef]
4. Ehrlich, H.L.; Newman, D.K.; Kappler, A. *Ehrlich's Geomicrobiology*, 6th ed.; CRC Press: Boca Raton, FL, USA, 2015; p. 635.
5. Johnston, C.W.; Wyatt, M.A.; Li, X.; Ibrahim, A.; Shuster, J.; Southam, G.; Magarvey, N. Gold biomineralization by a secondary metabolite from a gold-associated microbe. *Nat. Chem. Biol.* **2013**, *9*, 241–243. [CrossRef] [PubMed]
6. Nies, D.H. Microbial heavy-metal resistance. *Appl. Microbiol. Biotechnol.* **1999**, *51*, 730–750. [CrossRef] [PubMed]
7. Silver, S. Bacterial resistances to toxic metal ions—A review. *Gene* **1996**, *179*, 9–19. [CrossRef]
8. Mossman, D.J.; Dyer, B.D. The geochemistry of Witwatersrand-type gold deposits and the possible influence of ancient prokaryotic communities on gold dissolution and precipitation. *Precambrian Res.* **1985**, *30*, 303–319. [CrossRef]
9. Reith, F.; Lengke, M.F.; Falconer, D.; Craw, D.; Southam, G. Winogradsky review: The geomicrobiology of gold. *ISME J.* **2007**, *1*, 567–584. [CrossRef] [PubMed]
10. Shuster, J.; Southam, G. The in-vitro "growth" of gold grains. *Geology* **2015**, *43*, 79–82. [CrossRef]
11. Shuster, J.; Johnston, C.W.; Magarvey, N.A.; Gordon, R.A.; Barron, K.; Banerjee, N.R.; Southam, G. Structural and chemical characterization of placer gold grains: Implications for bacterial contributions to grain formation. *Geomicrobiol. J.* **2015**, *32*, 158–169. [CrossRef]

12. Southam, G.; Lengke, M.F.; Fairbrother, L.; Reith, F. The biogeochemistry of gold. *Elements* **2009**, *5*, 303–307. [CrossRef]
13. Lengke, M.F.; Fleet, M.E.; Southam, G. Morphology of gold nanoparticles synthesized by filamentous cyanobacteria from gold (I)-thiosulphate and gold (III)-chloride complexes. *Langmuir* **2006**, *22*, 2780–2787. [CrossRef] [PubMed]
14. Reith, F.; Rogers, S.L.; McPhail, D.C.; Webb, D. Biomineralization of gold: Biofilms on bacterioform gold. *Science* **2006**, *313*, 233–235. [CrossRef] [PubMed]
15. Reith, F.; Etschmann, B.; Grosse, C.; Moors, H.; Benotmane, M.A.; Monsieurs, P.; Grass, G.; Doonan, C.; Vogt, S.; Lai, B.; et al. Mechanisms of gold biomineralization in the bacterium *Cupriavidus metallidurans*. *Proc. Natl. Acad. Sci. USA* **2009**, *106*, 17757–17762. [CrossRef] [PubMed]
16. Tsuruta, T. Biosorption and recycling of gold using various microorgamisms. *J. Gen. Appl. Microbiol.* **2004**, *50*, 221–228. [CrossRef] [PubMed]
17. Kenney, J.P.L.; Song, Z.; Bunker, B.A.; Fein, J.B. An experimental study of Au removal from solution by non-metabolizing bacterial cells and their exudates. *Geochim. Cosmochim. Acta* **2012**, *87*, 51–60. [CrossRef]
18. Minter, W.E.L.; Goedhart, M.; Knight, J.; Frimmel, H.E. Morphology of Witwatersrand gold grains from the Basal Reef, evidence for their detrital origin. *Econ. Geol.* **1993**, *88*, 237–248. [CrossRef]
19. Wilson, A.F. Origin of quartz-free gold nuggets and supergene gold found in laterites and soils—A review and some new observations. *Aust. J. Earth Sci.* **1984**, *31*, 303–316.
20. Goldschmidt, V.M. *Geochemistry*; Oxford University Press: Oxford, UK, 1954; p. 730.
21. Maier, W.D. Pt-group element (PGE) deposits and occurrences: Mineralization styles, genetic concepts, and exploration criteria. *J. Afr. Earth Sci.* **2005**, *41*, 165–191. [CrossRef]
22. Mungall, J.E.; Naldrett, A.J. Ore deposits of the platinum-group elements. *Elements* **2008**, *4*, 253–258. [CrossRef]
23. Cabral, A.R.; Beaudoin, G.; Choquette, M.; Lehmann, B.; Polonia, J.C. Supergene leaching and formation of platinum in alluvium: Evidence from Serro, Minas Gerais, Brazil. *Mineral. Petrol.* **2007**, *90*, 141–150. [CrossRef]
24. Campbell, G.; Reith, F.; Etschmann, B.; Brugger, J.; Gordon, R.A.; Martinez-Criado, G.; Southam, G. Surface transformations of platinum grains from New South Wales, Australia. *Am. Mineral.* **2015**, *100*, 1236–1243. [CrossRef]
25. Reith, F.; Zammit, C.; Shar, S.S.; Etschmann, B.; Bottrill, R.; Southam, G.; Ta, C.; Kilburn, M.; Oberthür, T.; Ball, A.S.; et al. Biological role in the transformation of platinum-group mineral grains. *Nat. Geosci.* **2016**, *9*, 294–299. [CrossRef]
26. Macdonald, A.J. Ore deposit models #12: The platinum group element deposits—Classification and genesis. *Geosci. Can.* **1987**, *14*, 155–166.
27. Nixon, G.T.; Hammack, J.L. Metallogeny of ultramafic-mafic rocks in British Columbia with emphasis on the platinum-group elements. In *Ore Deposits, Tectonics, and Metallogeny in the Canadian Cordillera*; McMillan, W.J., Ed.; Province of British Columbia-Ministry of Energy, Mines and Petroleum Resources: Vancouver, BC, Canada, 1991; pp. 125–161, Paper 4.
28. Koek, M.; Kreuzer, O.P.; Maier, W.D.; Porwal, A.K.; Thompson, M.; Guj, P.A. Review of the PGM industry, deposit models and exploration practices: Implications for Australia's PGM potential. *Resour. Policy* **2010**, *35*, 20–35. [CrossRef]
29. Mountain, B.W.; Wood, S.A. Chemical controls on the solubility, transport and deposition of platinum and palladium in hydrothermal solutions, a thermodynamic approach. *Econ. Geol.* **1988**, *83*, 492–510. [CrossRef]
30. Colombo, C.; Oates, C.J.; Monhemius, A.J.; Plant, J.A. Complexation of platinum, palladium and rhodium with inorganic ligands in the environment. *Geochem. Explor. Environ. Anal.* **2008**, *8*, 91–101. [CrossRef]
31. Reith, F.; Campbell, S.G.; Ball, A.S.; Pring, A.; Southam, G. Platinum in earth surface environments. *Earth Sci. Rev.* **2014**, *131*, 1–21. [CrossRef]
32. Wood, S.A. The interaction of dissolved platinum with fulvic acid and simple organic acid analogues in aqueous solutions. *Can. Mineral.* **1990**, *28*, 665–673.
33. Anthony, E.Y.; Williams, P.A. Thiosulfate complexing of platinum group elements: Implications for supergene chemistry. In *Environmental Geochemistry of Sulfide Oxidation*; Alpers, C.N., Bowles, D.W., Eds.; American Chemical Society Books: Washington, DC, USA, 1994; pp. 551–560.

34. Azaroual, M.; Romand, B.; Freyssinet, P.; Disnar, J. Solubility of platinum in aqueous solutions at 25 °C and pHs 4 to 10 under oxidizing conditions. *Geochim. Cosmochim. Acta* **2001**, *65*, 4453–4466. [CrossRef]
35. Hanley, J.J. The aqueous geochemistry of the Platinum-Group Elements (PGE) in surficial, low-T hydrothermal and high-T magmatic-hydrothermal environments. In *Exploration for Platinum-Group Element Deposits*; Mungall, J.E., Ed.; Mineralogical Association of Canada: Ottawa, ON, Canada, 2005; pp. 35–56.
36. Vlassopoulos, D.; Wood, S.A.; Mucci, A. Gold speciation in natural waters: II. The importance of organic complexing-experiments with some simple model ligands. *Geochim. Cosmochim. Acta* **1990**, *54*, 1575–1586. [CrossRef]
37. Bowles, J.F.W. The development of platinum-group minerals in laterites. *Econ. Geol.* **1986**, *81*, 1278–1285. [CrossRef]
38. Lengke, M.F.; Fleet, M.E.; Southam, G. Synthesis of platinum nanoparticles by reaction of filamentous cyanobacteria with platinum(IV)−chloride complex. *Langmuir* **2006**, *22*, 7318–7323. [CrossRef] [PubMed]
39. Konishi, Y.; Ohnoa, K.; Saitoh, N.; Nomura, T.; Nagamine, S.; Hishida, H.; Takahashi, Y.; Uruga, T. Bioreductive deposition of platinum nanoparticles on the bacterium *Shewanella algae*. *J. Biotechnol.* **2007**, *128*, 648–653. [CrossRef] [PubMed]
40. Cabral, A.R.; Radtke, M.; Munnik, F.; Lehmann, B.; Reinholz, U.; Riesemeier, H.; Tupinambá, M.; Kwitko-Ribeiro, R. Iodine in alluvial platinum–palladium nuggets: Evidence for biogenic precious-metal fixation. *Chem. Geol.* **2011**, *281*, 125–132. [CrossRef]
41. Guiné, V.; Martins, J.M.F.; Causse, B.; Durand, A.; Gaudet, J.P.; Spadini, L. Effect of cultivation and experimental conditions on the surface reactivity of the metal-resistant bacteria *Cupriavidus metallidurans* CH34 to protons, cadmium and zinc. *Chem. Geol.* **2007**, *236*, 266–280. [CrossRef]
42. Mergeay, M.; Nies, D.; Schlegel, H.G.; Gerits, J.; Charles, P.; Van Gijsegem, F. *Alicaligenes eutrophus* CH34 is a facultative chemolithotroph with plasmid-bound resistance to heavy metals. *J. Bacteriol.* **1985**, *62*, 328–334.
43. Mergeay, M.; Monchy, S.; Vallaeys, T.; Auquier, V.; Benotmane, A.; Bertin, P.; Taghavi, S.; Dunn, J.; van der Lelie, D.; Wattiez, R. *Ralstonia metallidurans*, a bacterium specifically adapted to toxic metals: Towards a catalogue of metal-responsive genes. *FEMS Microbiol. Rev.* **2003**, *27*, 385–410. [CrossRef]
44. Ledrich, M.; Stemmler, S.; Laval-Gilly, P.; Foucaud, L.; Falla, J. Precipitation of silver-thiosulphate complex and immobilization of silver by *Cupriavidus metallidurans* CH34. *BioMetals* **2005**, *18*, 643–650. [CrossRef] [PubMed]
45. Sanders, E.R. Aseptic laboratory techniques: Plating methods. *J. Vis. Exp.* **2012**, *63*, e3064. [CrossRef] [PubMed]
46. Baldwin, M.; Bankston, P. Measurement of live bacteria by Nomarski interference microscopy and steriologic methods as tested by macroscopic rod-shaped models. *Appl. Environ. Microbiol.* **1988**, *54*, 105–109. [PubMed]
47. Williams, G.P. Electron binding energies. In *X-ray Data Booklet*; Thompson, A.C., Vaughan, D., Eds.; Lawrence Berkeley National Laboratory, University of California: Berkeley, CA, USA, 2001; Section 1.1.
48. Ravel, B.; Newville, M. ATHENA, ARTEMIS, HEPHAESTUS: Data analysis for X-ray absorption spectroscopy using IFEFFIT. *J. Synchrotron Radiat.* **2005**, *12*, 537–541. [CrossRef] [PubMed]
49. Goldberg, S.; Doyle, J.; Rosenberg, M. Mechanism of enhancement of microbial cell hydrophobicity by cationic polymers. *J. Bacteriol.* **1990**, *172*, 5650–5654. [CrossRef] [PubMed]
50. Ohba, S.; Sato, S.; Saito, Y. Electron-density distribution in crystals of potassium tetrachloroplatinate (II) and influence of X-ray diffuse scattering. *Acta Crystallogr. Sect. B* **1983**, *39*, 49–53. [CrossRef]
51. Moret, M.E.; Keller, S.F.; Slootweg, J.C.; Chen, P. Mononuclear platinum (II) complexes incorporating κ^2-carboxylate ligands: Synthesis, structure, and reactivity. *Inorg. Chem.* **2009**, *48*, 6972–6978. [CrossRef] [PubMed]
52. Ankudinov, A.L.; Rehr, J.J.; Bare, S.R. Hybridization peaks in Pt-Cl XANES. *Chem. Phys. Lett.* **2000**, *316*, 495–500. [CrossRef]
53. Wood, S.A.; Mountain, B.W.; Pan, P. The aqueous geochemistry of platinum, palladium and gold: Recent experimental constraints and a re-evaluation of theoretical predictions. *Can. Mineral.* **1992**, *30*, 955–982.
54. Beveridge, T.J.; Murray, R.G.E. Sites of metal deposition in the cell wall of *Bacillus subtilis*. *J. Bacteriol.* **1980**, *141*, 876–887. [PubMed]
55. Guiné, V.; Spadini, L.; Sarret, G.; Muris, M.; Delolme, C.; Gaudet, J.P.; Martins, J.M.F. Zinc sorption to three gram-negative bacteria: Combined titration, modeling, and EXAFS study. *Environ. Sci. Technol.* **2006**, *40*, 1806–1813. [CrossRef] [PubMed]

56. Fein, J.; Daughney, C.; Yee, N.; Davis, T.A. Chemical equilibrium model for metal adsorption onto bacterial surfaces. *Geochim. Cosmochim. Acta* **1997**, *61*, 3319–3328. [CrossRef]
57. Kubrakova, I.V.; Fortygin, A.V.; Lobov, S.G.; Koshcheeva, I.Y.; Tyutyunnik, O.A.; Mironenko, M.V. Migration of platinum, palladium, and gold in the water systems of platinum deposits. *Geochem. Int.* **2011**, *49*, 1072–1084. [CrossRef]
58. Janssen, P.J.; Van Houdt, R.; Moors, H.; Monsieurs, P.; Morin, N.; Michaux, A.; Benotmane, M.A.; Leys, N.; Vallaeys, T.; Lapidus, A.; et al. The complete genome sequence of *Cupriavidus metallidurans* strain CH34, a master survivalist in harsh and anthropogenic environments. *PLoS ONE* **2010**, *5*, e10433. [CrossRef] [PubMed]
59. Urrutia, M.; Kemper, M.; Doyle, R.; Beveridge, T.J. The membrane-induced proton motive force influences the metal binding ability of *Bacillus subtilis* cell walls. *Appl. Environ. Microbiol.* **1992**, *58*, 3837–3844.
60. Etschmann, B.; Brugger, J.; Fairbrother, L.; Grosse, C.; Nies, D.H.; Martinez-Criado, G.; Reith, F. Applying the Midas touch: Differing toxicity of mobile gold and platinum complexes drives biomineralization in the bacterium *Cupriavidus metallidurans*. *Chem. Geol.* **2016**, *438*, 103–111. [CrossRef]
61. Fuchs, W.A.; Rose, A.W. The geochemical behavior of platinum and palladium in the weathering cycle in the Stillwater Complex, Montana. *Econ. Geol.* **1974**, *69*, 332–346. [CrossRef]

© 2018 by the authors. Licensee MDPI, Basel, Switzerland. This article is an open access article distributed under the terms and conditions of the Creative Commons Attribution (CC BY) license (http://creativecommons.org/licenses/by/4.0/).